Electronic Supplementary Material (ESI) for Environmental Science: Water Research & Technology.

ESI

# Transport mechanisms of water molecules and ions in sub-nano channels of nanostructured water treatment liquid-crystalline membranes: a molecular dynamics simulation study

Hiroki Nada,*[a] Takeshi Sakamoto,[b] Masahiro Henmi,[c] Takafumi Ogawa,[d] Masahiro Kimura,[d] and Takashi Kato*[b]

[a] National Institute of Advanced Industrial Science and Technology (AIST), 16-1 Onogawa, Tsukuba, Ibaraki 305-8569, Japan. E-mail: hiroki.nada@aist.go.jp

[b] Department of Chemistry and Biotechnology, School of Engineering, The University of Tokyo, Hongo, Bunkyo-ku, Tokyo 113-8656, Japan. E-mail: kato@chiral.t.u-tokyo.ac.jp

[c] Technology Center, Toray Industries, Inc., 1-1, Nihonbashi-Muromachi 2-chome, Chuo-ku, Tokyo 103-8666, Japan.

[d] Global Environment Research Laboratories, Toray Industries, Inc., Sonoyama, Otsu, Shiga 520-0842, Japan.

## S1. Simulation Method

### S1-1. Simulation systems

Following the previous molecular dynamics (MD) simulation study [S1], a simulation system including a sub-nanometer channel formed by LC compounds was constructed using a simplified model of LC compounds from which the alkoxy chains of the nonionic moiety were eliminated (LC monomer). First, an LC tetramer layer was formed with four LC monomers (Fig. S1a). In this layer, the LC monomers were arranged radially at positions rotated by 90°, such that their ammonium moieties were oriented toward the center of the layer. The distances between the center of the channel and the benzene rings of the LC monomers in the $x$–$y$ plane, $R$, were set to be the most energetically stable of 1.0 nm for **1** and 0.825 nm for **2**, which were determined in the previous MD simulation study [S1].

Second, an assembly of four LC tetramer layers was constructed to create a sub-nanometer channel at the center by stacking the layers in the $z$ direction (Fig. S1b). In the assembly, the second and fourth layers were rotated by 45° around the center to form a close-packed structure. The distance between the layers was set to the experimental value of 0.45 nm [S1]. To make the assembly electrically neutral, 16 counter $Cl^-$ ions were inserted into the channel of the assembly. The assembly was put into a rectangular parallelepiped with the dimensions of $5.0 \times 5.0 \times 1.8$ nm$^3$ so that the channel axis was parallel to the $z$-axis (Fig. S1c). This rectangular parallelepiped system in which periodic boundary conditions were imposed in all $x$, $y$, and $z$ directions (unit system) was used for a grand canonical Monte Carlo (GCMC) simulation to determine the number of water molecules in the channel. Using the final configuration generated by the GCMC simulation, the system for the MD simulations (simulation system) was constructed by putting a copy of the unit system filled with water molecules onto the original system in the $z$-axis direction.

Because we focused on the mobility of water molecules and ions in the channel, water molecules and ions far from the channel were eliminated from the simulation system. A water molecule was judged to be far from the channel if it was not included in a circular column with a radius of $R$ from the center of the channel.

### S1-2. Potential models

The intermolecular interactions of the LC monomers were estimated as the sum of intermolecular potentials (Coulomb and Lennard-Jones (LJ) potentials [$= 4\varepsilon\{(\sigma/r)^{12} - (\sigma/r)^6\}$, where $r$ is the distance between a pair of sites]) for all atoms of the LC monomer plus the sum of intramolecular potentials (bond, valent angle, and dihedral angle potentials). Parameters of these potentials for each LC compound, which were determined in the previous MD simulation study [S1], were used in this study. As with the previous MD simulation study [S1], the TIP3P model [S2] was used to estimate the interaction between a pair of water molecules, and the interactions of the $Na^+$ and $Cl^-$ ions were estimated using a model proposed by Joung and Cheatham [S3]. The interactions of the $NO_3^-$ ions were calculated using a model proposed by Banerjee et al. [S4] because it reproduces the real hydration structure of an $NO_3^-$ ion. In this model, an $NO_3^-$ ion is a planar rigid rotor with an N–O distance of 0.1226 nm and an O–N–O angle of 120°. The definitions of the atomic sites of the LC monomers are given in Fig. S2. Potential parameters for water molecules and ions and potential parameters for the LC monomers are given in Tables S1 and S2, respectively.

The interaction between the LC monomer and the water molecules, and $Na^+$, $Cl^-$, and $NO_3^-$ ions was represented as the sum of the Coulomb potentials plus the sum of the LJ potentials. The parameters, $\varepsilon$ and $\sigma$, between them were determined by the Lorentz-Berthelot rules. As with the previous MD simulation study [S1], $\sigma$ for the interaction between the LC monomer and each of the ions, which was determined by the Lorentz-Berthelot rules, was multiplied by 0.9 to reduce the deviation from the potential energy between them, which was calculated using the MP2 method with the 6-311+G** basis function.

### S1-3. GCMC simulation

The GCMC simulation was performed for the unit system to fill the system with water molecules. The temperature was set to 298 K and the chemical potential was set to the value for the bulk water at 298 K and 10 atm in the TIP3P model (−26 kJ/mol). The total number of trials (translation, rotation, insertion, and removal of water molecules) was $1.4 \times 10^{10}$.

### S1-4. MD simulation

A standard MD simulation for the NVT ensemble was performed for each of systems **1** and **2**. Several earlier simulation studies for water desalination used a nonequilibrium MD (NEMD) simulation [S5] to create a flow of a solution in water treatment materials under external pressure [S6-S9]. However, the flow rate in real LC membranes is low; the experimental flux value of an NaCl solution through the LC membrane is 50 L $m^{-2}$ $h^{-1}$ [S10]. A run of an NEMD simulation, which is typically on the order of a microsecond or less, is not sufficient to reproduce the low flow rate in real LC membranes. Thus, in this study, we performed the MD simulation in the equilibrium state, and the mobilities of water molecules and ions in the channel were evaluated by analyzing the mean square displacements, $\langle dr^2 \rangle$, as a function of time, $t$, and the number density profiles, $\rho$, of water molecules and ions along the $z$-axis direction.

Computation was carried out by a leap-frog algorithm with a time step of 0.5 fs [S5]. The simulation for each system was performed three times starting with different initial positions of $Na^+$ and $Cl^-$ or $NO_3^-$ ions in the solution. Each simulation run was 15 ns. The simulation data for a period of 1 ns from the beginning of the simulation was used for the equilibration of the system, and the simulation data for the subsequent 14 ns was used to analyze the mobilities of the water molecules and ions in the channel. The temperature was maintained at 298 K using a Nosé-Hoover thermostat with a coupling parameter of 0.1 ps [S11]. The C-H distances in the LC monomer were kept constant at their equilibrium values by the SHAKE algorithm [S12]. The Ewald summation method was used to estimate the long-range Coulomb interactions. The convergence parameter for the Ewald method was set to 3.208 $nm^{-1}$, the real space cut-off distance was set to 1 nm, and the numbers of reciprocal vectors were 16, 16, and 12. The MD simulation was performed with DL_POLY 2.20 [S13].

During the simulation, an external cylindrical wall potential, $\phi = A(R - r_{xy})^{-n}$, was applied to the system to prevent water molecules and ions from moving out of the channel, where $A = 1.0 \times 10^{-3}$ kJ/mol and $n = 4$. $r_{xy}$ was the distance between the center of the channel and species in the $x$–$y$ plane. The numbers of water molecules inside the cylindrical wall were 162 in system **1** and 148 for both solutions in system **2**. The mobility analysis was only performed for the water molecules and ions in a cylinder with a radius of the distance between the N1 atom, which was the N atom of the LC monomer, and the center of the channel in the $x$–$y$ plane.

### S1-5. Metadynamics method

The metadynamics (MTD) method is an enhanced sampling method that increases the probability of visiting high free-energy states by adding a bias potential, which is a function of collective variables (CVs), to the minima of the potential energy surface of the system [S14-S17]. In this study, the position of the $Na^+$ ion along the $x$-axis and that along the $z$-axis were chosen as CVs. To create the free-energy landscape of the $Na^+$ ion in the channel by the MTD method, the MD simulation was performed by implementing PLUMED 1.3 [S16] in DL_POLY 2.20 [S13]. The well-tempered MTD method [S18] was used to obtain the free-energy landscape with sufficiently high accuracy. The bias potential for the MTD method was represented as a function of Gaussians. The height of the Gaussians was set to 3.0 kJ/mol, and the sigma parameter of the Gaussians was set to 0.035 nm. The bias potential was added to the Hamiltonian of the system at every 100 MD steps. The bias factor parameter in the well-tempered MTD method was set to 10. The total run of the simulation was 40 ns.

## S2. MD Simulations for the Bulk Solutions

The MD simulations for the bulk NaCl and $NaNO_3$ solutions were performed using the same potential models of water molecules and ions as in the simulation of the solution in the channel. The simulation system of the MD simulation for each bulk solution was a rectangular parallelepiped consisting of 998 water molecules, one $Na^+$ ion, and one $Cl^-$ or $NO_3^-$ ion. Periodic boundary conditions were imposed in all three directions of the system. Computation was carried out by a leap-frog algorithm with a time step of 1.0 fs [S5]. The total run was 15 ns. The data for 5 ns from the beginning of the simulation were discarded as an equilibration period and the data for the subsequent 10 ns were used for the analysis of $g_{\mathrm{OwOw}}$. Temperature and pressure were maintained at 298 K and 10 atm, respectively, by a method proposed by Berendsen *et al.* [S19]. The thermal and pressure bath constants were set to 0.1 and 2.0 ps, respectively. The Ewald summation method was used to estimate the long-range Coulomb interaction. The convergence parameter for the Ewald method was set to 3.208 $nm^{-1}$ and the real space cut-off distance was set to 1 nm. The MD simulation was performed with DL_POLY 2.20 [S13].

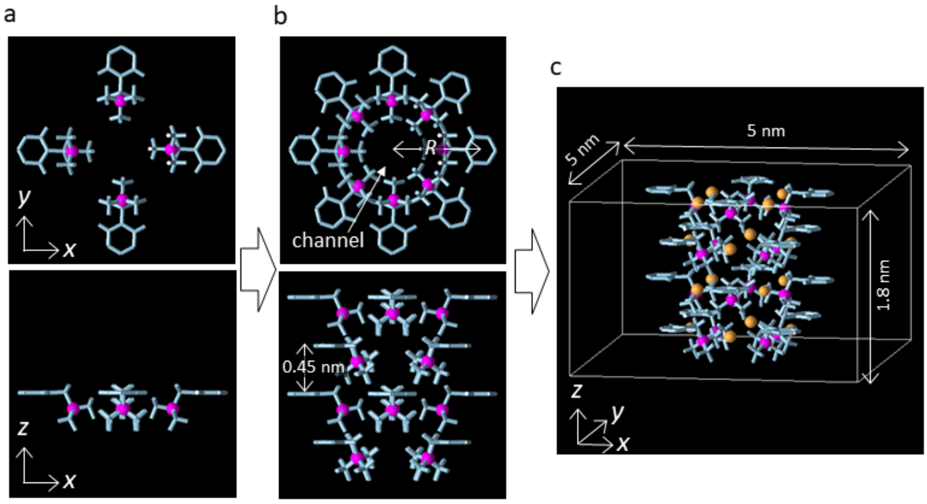

**Fig. S1** Procedure for creating the unit system for system **2**. (a) LC tetramer layer formed from four LC monomers. (b) Assembly of four LC tetramer layers. (c) Unit system used for the GCMC simulations. In the lower panels, only the interatomic bonds (light blue columns) and the N atom (magenta spheres) of the LC monomers and the counter $Cl^-$ ions (chrome yellow spheres) are shown. This figure is reproduced from Figure S13 in the Supporting Information of our previous paper [S1].

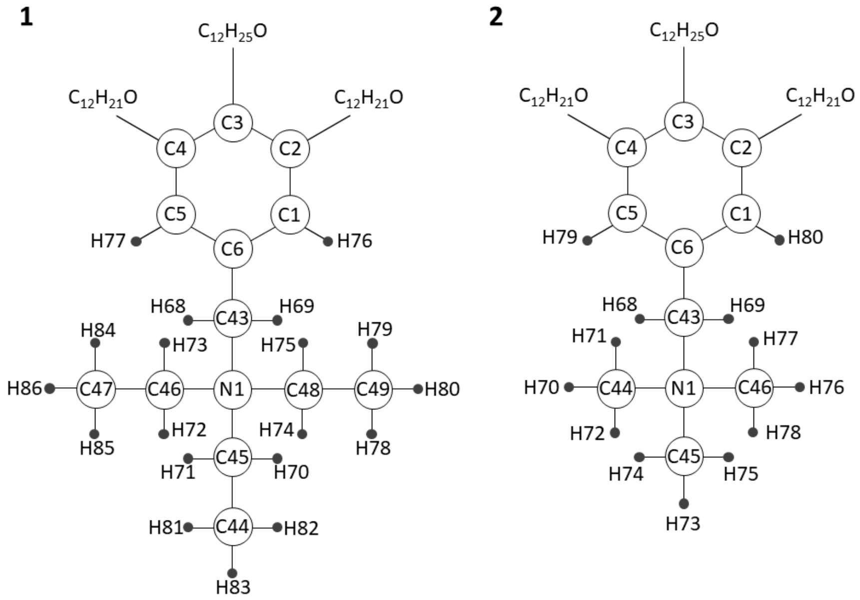

**Fig. S2** Definitions of the atomic sites in LC monomers **1** and **2**. This figure is reproduced from the Supporting Information of our previous paper [S1]. LC compounds **1** and **2** in the present paper, respectively, correspond to LC compounds ***1*(*n*)** and ***3*(*n*)** in the previous paper.

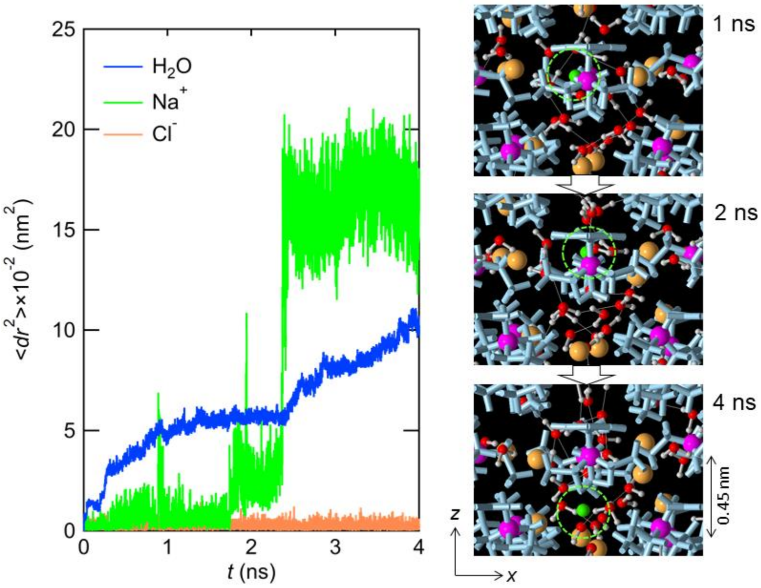

**Fig. S3** $\langle dr^2 \rangle$ as a function of $t$ for the NaCl solution and snapshots for the $Na^+$ (green sphere) in the channel at 1, 2, and 4 ns. The $\langle dr^2 \rangle$ function was created without averaging the functions created with the simulation data for different periods. The sudden increases of $\langle dr^2 \rangle$ for $Na^+$ at 1.8 and 2.4 ns indicate jump diffusion.

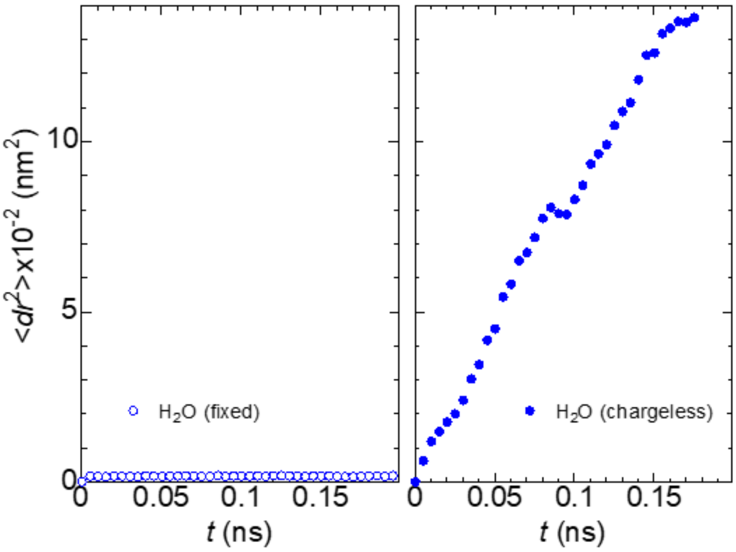

**Fig. S4** $\langle dr^2 \rangle$ as a function of $t$ for water molecules of the NaCl solution in system **1** under the fixed and chargeless conditions. The $\langle dr^2 \rangle$ function for each condition was obtained with an NEMD simulation. During the simulation, a constant force of 0.425 kJ/mol Å$^{-1}$ was applied to the $z$ direction of each water molecule and each ion in the system. For the chargeless condition, the mobility of water molecules significantly increased by applying the constant force, because the interaction between the channel wall and each of the water molecules was weak.

**Table S1** Charge ($q$) and LJ parameters ($\varepsilon$ and $\sigma$) of the LJ potential ($= 4\varepsilon\{(\sigma/r)^{12} - (\sigma/r)^6\}$, where $r$ is the distance between a pair of sites) for $Na^+$, $Cl^-$, $H_2O$, and $NO_3^-$. Ow and Hw are the O and H atoms of $H_2O$, respectively. Nn and On are the N and O atoms of $NO_3^-$, respectively.

| | $Na^{+\,a}$ | $Cl^{-\,a}$ | $H_2O$ [b] | | $NO_3^{-\,c}$ | |
|---|---|---|---|---|---|---|
| | | | Ow | Hw | Nn | On |
| $q$ ($e$C) | +1 | −1 | +0.834 | −0.417 | +1.118 | −0.706 |
| $\varepsilon$ (kJ/mol) | 0.366 | 0.149 | 0.636 | — | 0.711 | 0.837 |
| $\sigma$ (nm) | 0.2439 | 0.4478 | 0.3151 | — | 0.315 | 0.285 |

[a] Ref. [S3] [b] Ref. [S2] [c] Ref. [S4]

**Table S2** $q$, $\varepsilon$, and $\sigma$ for LC compounds **1** and **2**. This table is reproduced from the Supporting Information of our previous paper [S1].

| **1** | C1 | C2 | C3 | C4 | C5 | C6 | N11 |
|---|---|---|---|---|---|---|---|
| $q$ ($e$C) | -0.293297 | 0.063165 | -0.004115 | 0.260638 | -0.293297 | 0.064509 | -0.152894 |
| $\varepsilon$ (kJ/mol) | 0.3598 | 0.3598 | 0.3598 | 0.3598 | 0.3598 | 0.3598 | 0.7113 |
| $\sigma$ (nm) | 0.3400 | 0.3400 | 0.3400 | 0.3400 | 0.3400 | 0.3400 | 0.3250 |
| | | | | | | | |
| | C43 | H68 | H69 | C44 | C45 | H70 | H71 |
| $q$ ($e$C) | -0.194313 | 0.151863 | 0.151863 | 0.110138 | 0.110138 | 0.060731 | 0.060731 |
| $\varepsilon$ (kJ/mol) | 0.4577 | 0.0657 | 0.0657 | 0.4577 | 0.4577 | 0.0657 | 0.0657 |
| $\sigma$ (nm) | 0.3400 | 0.1960 | 0.1960 | 0.3400 | 0.3400 | 0.1960 | 0.1960 |
| | | | | | | | |
| | H72 | C46 | C47 | H73 | H74 | C48 | H75 |
| $q$ ($e$C) | 0.060731 | -0.177088 | -0.177088 | 0.060731 | 0.187759 | 0.110138 | 0.187759 |
| $\varepsilon$ (kJ/mol) | 0.0657 | 0.4577 | 0.4577 | 0.0657 | 0.0657 | 0.4577 | 0.0657 |
| $\sigma$ (nm) | 0.1960 | 0.3400 | 0.3400 | 0.1960 | 0.1960 | 0.3400 | 0.1960 |
| | | | | | | | |
| | C49 | H76 | H77 | H78 | H79 | H80 | H81 |
| $q$ ($e$C) | -0.177088 | 0.078536 | 0.078536 | 0.078536 | 0.078536 | 0.078536 | 0.078536 |
| $\varepsilon$ (kJ/mol) | 0.4577 | 0.0628 | 0.0628 | 0.0657 | 0.0657 | 0.0657 | 0.0657 |
| $\sigma$ (nm) | 0.3400 | 0.2600 | 0.2600 | 0.2650 | 0.2650 | 0.2650 | 0.2650 |
| | | | | | | | |
| | H82 | H83 | H84 | H85 | H86 | | |
| $q$ ($e$C) | 0.060731 | 0.060731 | 0.078536 | 0.078536 | 0.078536 | | |
| $\varepsilon$ (kJ/mol) | 0.0657 | 0.0657 | 0.0657 | 0.0657 | 0.0657 | | |
| $\sigma$ (nm) | 0.2650 | 0.2650 | 0.2650 | 0.2650 | 0.2650 | | |

| **2** | C1 | C2 | C3 | C4 | C5 | C6 | C43 |
|---|---|---|---|---|---|---|---|
| $q$ ($e$C) | -0.308209 | 0.277377 | -0.217685 | 0.277377 | -0.308209 | 0.053544 | -0.094756 |
| $\varepsilon$ (kJ/mol) | 0.3598 | 0.3598 | 0.3598 | 0.3598 | 0.3598 | 0.3598 | 0.4577 |
| $\sigma$ (nm) | 0.3400 | 0.3400 | 0.3400 | 0.3400 | 0.3400 | 0.3400 | 0.3400 |
| | | | | | | | |
| | C44 | C45 | C46 | N1 | H68 | H69 | H70 |
| $q$ ($e$C) | -0.327552 | -0.327552 | -0.327552 | 0.134496 | 0.127527 | 0.127527 | 0.171085 |
| $\varepsilon$ (kJ/mol) | 0.4577 | 0.4577 | 0.4577 | 0.7113 | 0.0657 | 0.0657 | 0.0657 |
| $\sigma$ (nm) | 0.3400 | 0.3400 | 0.3400 | 0.3250 | 0.1960 | 0.1960 | 0.1960 |
| | | | | | | | |
| | H71 | H72 | H73 | H74 | H75 | H76 | H77 |
| $q$ ($e$C) | 0.171085 | 0.171085 | 0.171085 | 0.171085 | 0.171085 | 0.171085 | 0.171085 |
| $\varepsilon$ (kJ/mol) | 0.0657 | 0.0657 | 0.0657 | 0.0657 | 0.0657 | 0.0657 | 0.0657 |
| $\sigma$ (nm) | 0.1960 | 0.1960 | 0.1960 | 0.1960 | 0.1960 | 0.1960 | 0.1960 |
| | | | | | | | |
| | H78 | H79 | H80 | | | | |
| $q$ ($e$C) | 0.171085 | 0.186951 | 0.186951 | | | | |
| $\varepsilon$ (kJ/mol) | 0.0657 | 0.0628 | 0.0628 | | | | |
| $\sigma$ (nm) | 0.1960 | 0.2600 | 0.2600 | | | | |

## References

S1. T. Sakamoto, T. Ogawa, H. Nada, K. Nakatsuji, M. Mitani, B. Soberats, K. Kawata, M. Yoshio, H. Tomioka, T. Sasaki, M. Kimura, M. Henmi and T. Kato, Development of nanostructured water treatment membranes based on thermotropic liquid crystals: Molecular design of sub-nanoporous materials, *Adv. Sci.*, 2018, **5**, 9.

S2. W. L. Jorgensen, J. Chandrasekhar, J. D. Madura, R. W. Impey and M. L. Klein, Comparison of simple potential functions for simulating liquid water, *J. Chem. Phys.*, 1983, **79**, 926-935.

S3. I. S. Joung and T. E. Cheatham, Determination of alkali and halide monovalent ion parameters for use in explicitly solvated biomolecular simulations, *J. Phys. Chem. B*, 2008, **112**, 9020-9041.

S4. P. Banerjee, S. Yashonath and B. Bagchi, Coupled jump rotational dynamics in aqueous nitrate solutions, *J. Chem. Phys.*, 2016, **145**, 10.

S5. M. P. Allen and D. J. Tildesley, *Computer Simulation of Liquids*, Clarendon Press, Oxford, 1989.

S6. M. X. Ding, A. Szymczyk and A. Ghoufi, On the structure and rejection of ions by a polyamide membrane in pressure-driven molecular dynamics simulations, *Desalination*, 2015, **368**, 76-80.

S7. L. Y. Wang, R. S. Dumont and J. M. Dickson, Nonequilibrium molecular dynamics simulation of water transport through carbon nanotube membranes at low pressure, *J. Chem. Phys.*, 2012, **137**, 14.

S8. H. Ebro, Y. M. Kim and J. H. Kim, Molecular dynamics simulations in membrane-based water treatment processes: A systematic overview, *J. Membr. Sci.*, 2013, **438**, 112-125.

S9. L. Y. Wang, R. S. Dumont and J. M. Dickson, Molecular dynamic simulations of pressure-driven water transport through polyamide nanofiltration membranes at different membrane densities, *RSC Adv.*, 2016, **6**, 63586-63596.

S10. M. Henmi, K. Nakatsuji, T. Ichikawa, H. Tomioka, T. Sakamoto, M. Yoshio and T. Kato, Self-organized liquid-crystalline nanostructured membranes for water treatment: Selective permeation of ions, *Adv. Mater.*, 2012, **24**, 2238-2241.

S11. W. G. Hoover, Canonical dynamics - equilibrium phase-space distributions, *Phys. Rev. A*, 1985, **31**, 1695-1697.

S12. J. P. Ryckaert, G. Ciccotti and H. J. C. Berendsen, Numerical-integration of cartesian equations of motion of a system with constraints - molecular-dynamics of n-alkanes, *J. Comput. Phys.*, 1977, **23**, 327-341.

S13. W. Smith and T. R. Forester, Dl_poly_2.0: A general-purpose parallel molecular dynamics simulation package, *Journal of Molecular Graphics*, 1996, **14**, 136-141.

S14. A. Laio and M. Parrinello, Escaping free-energy minima, *Proc. Natl. Acad. Sci. U. S. A.*, 2002, **99**, 12562-12566.

S15. A. Laio and F. L. Gervasio, Metadynamics: A method to simulate rare events and reconstruct the free energy in biophysics, chemistry and material science, *Rep. Prog. Phys.*, 2008, **71**, 22.

S16. M. Bonomi, D. Branduardi, G. Bussi, C. Camilloni, D. Provasi, P. Raiteri, D. Donadio, F. Marinelli, F. Pietrucci, R. A. Broglia and M. Parrinello, Plumed: A portable plugin for free-energy calculations with molecular dynamics, *Comput. Phys. Commun.*, 2009, **180**, 1961-1972.

S17. H. Nada, M. Kobayashi and M. Kakihana, Anisotropy in stable conformations of hydroxylate ions between the {001} and {110} planes of $TiO_2$ rutile crystals for glycolate, lactate, and 2-hydroxybutyrate ions studied by metadynamics method,*ACS Omega*, 2019, **4**, 11014-11024.

S18. A. Barducci, G. Bussi and M. Parrinello, Well-tempered metadynamics: A smoothly converging and tunable free-energy method, *Phys. Rev. Lett.*, 2008, **100**, 4.

S19. H. J. C. Berendsen, J. P. M. Postma, W. F. Vangunsteren, A. Dinola and J. R. Haak, Molecular-dynamics with coupling to an external bath, *J. Chem. Phys.*, 1984, **81**, 3684-3690.